High performance magnesium anode in paper-based microfluidic battery, powering on-chip fluorescence assay

Youngmi Koo, Jagannathan Sankar, and Yeoheung Yun[a)]
Engineering Research Center, Department of Chemical, Biological, and Bio Engineering, North Carolina A&T State University, Greensboro, North Carolina 27411, USA

(Received 16 July 2014; accepted 26 August 2014; published online 5 September 2014)

A high power density and long-lasting stable/disposable magnesium battery anode was explored for a paper-based fluidic battery to power on-chip functions of various Point of Care (POC) devices. The single galvanic cell with magnesium foil anode and silver foil cathode in Origami cellulose chip provided open circuit potential, 2.2 V, and power density, 3.0 mW/cm^2. A paper-based fluidic galvanic cell was operated with one drop of water (80 μl) and continued to run until it was dry. To prove the concept about powering on-chip POC devices, two-serial galvanic cells are developed and incorporated with a UV-light emitting diode ($\lambda = 365$ nm) and fluorescence assay for alkaline phosphatase reaction. Further, detection using smart phones was performed for quantitative measurement of fluorescent density. To conclude, a magnesium-based fluidic battery paper chip was extremely low-cost, required minute sample volumes, was easy to dispose of, light weight, easy to stack, store and transport, easy to fabricate, scalable, and has faster analysis times. © *2014 AIP Publishing LLC*. [http://dx.doi.org/10.1063/1.4894784]

I. INTRODUCTION

Since the discovery of thin film chromatography, paper-based technologies have recently been rediscovered and the challenges in those technologies taken up.[1–4] Paper-based technologies have applications in a wide range of fields, including analytical devices for medical diagnosis,[5–7] electronic circuits,[8] and batteries.[9–11] Batteries employing paper-based technologies are low-cost, lightweight, flexible, reliable, disposable, and biodegradable, which make them ideal power sources for point-of-care devices. In particular, battery-powered fluorescent detection on single paper-based fluidic chip can provide rapid/quantitative analysis and prevent possible contamination.[10,12]

Recently, Thom *et al*. and Esquivel *et al*.[10,11] demonstrated the feasibility of using a type of paper-based battery in a point of care device. However, these studies also highlight the challenges that remain in the implementation of such batteries, including achieving high power density, matching the life-time of the battery to its intended use and addressing the complexity of paper-based battery systems. To maximize energy efficiency in a paper-based electrochemical cell, parameters to be optimized include selection of anode/cathode electrodes, electrolyte, salt-bridge, paper-matrix materials, and fluidic design. Other challenges require resolution of similar numbers of parameters.

Magnesium is a promising metal anode due to its bivalency, highly negative Standard Reduction Potential (−2.37 vs. Normal-Hydrogen-Electrode (NHE)), specific charge capacity (2205 Ah/kg),[13] and high energy density (3.8 Ah/cm^3).[14] The use of magnesium in a disposable battery is attractive because of its low cost (~$2700/ton), abundance (the 5th most abundant element in the earth's crust), as well as its environmental stability, biocompatibility/biodegradability, low toxicity, and ease of handling.[15–20]

[a)]Author to whom correspondence should be addressed. Electronic mail: yyun@ncat.edu. Tel: (336) 285-3226. Fax: (336) 256-1153.

Here, we report a paper-based fluidic galvanic cell using magnesium as an anode in a cellulose paper device. The galvanic cell, with the addition of one drop of water, can provide sufficient power with a certain potential/current for a period of time, determined by the presence of water in the system. This time-limited activity means that the magnesium paper-based battery has great potential as a disposable device for emergency power supply and for the monitoring/diagnosing of drug abuse, bacterial, virus, biological/chemical defense, and ailments. In this paper, we integrate a paper-based battery into a chip containing an ultraviolet-light emitting diode (UV-LED) and fluorescent assay components. We show that alkaline phosphatase (ALP), which is an indicator of several diseases including liver diseases, liver cancer, hepatitis, bone disease, osteoblastic bone cancer, kidney cancer, and other ailments,[21,22] can be detected using a paper-based point of care device and a smartphone's application software.

II. MATERIALS AND METHODS

A. Chemicals and materials

Magnesium foil (99.5% purity, 2.50 mm wide, and 0.15 mm thick) was purchased from Alfa Aesar. Corrosion products were removed by chromate solution (ASTM G1–03-E, Standard Practice for Preparing, Cleaning, and Evaluating Corrosion Test Specimens, C.5.1) and polished sequentially with 600, 800, 1000, and 1200 grit silicon carbide sandpaper, followed by washing with ethanol and drying with nitrogen stream. Final dimensions of the magnesium anode were 2.50 mm × 6.50 mm × 0.10 mm. The polished magnesium foil was stored in desiccators until use. Silver foil (Alfa Aesar, 0.10 mm thickness, 99.998% pure, annealed) was polished according to the method for magnesium foil; the final dimensions of the cathode electrode was 2.50 mm × 6.50 mm × 0.08 mm. Other chemicals, magnesium chloride ($MgCl_2$, pure, ACROS organics), silver nitrate ($AgNO_3$, 99%, ACROS organics), and barium chromate ($BaCrO_4$, 99.998%, Alfa Aesar) were used as received. Chromatographic cellulose filter paper (Whatman grade 1, 0.18 mm thickness) was used for the battery structure, which typically had linear flow rate (water) of 130 mm/30 min. Red LED (RadioShack), glue stick (3M), polypropylene (PP) film (3M), and conductive pen (CircuitWriter™) were used in the construction of the battery. For the disclosed fluorescence assay, an endogenous phosphatase detection kit (Life technologies, ELF 97 Phosphatase detection kit, E6601), phosphatase (Sigma Aldrich, Alkaline from bovine intestinal mucosa), and 365 nm UV-LED (Nichia, NSSU100C) were employed.

B. Paper-based galvanic cell fabrication

Wax printing technology was used to fabricate paper-based fluidic galvanic cell devices. A design was created using AutoCAD (Fig. S1 in the supplementary material)[23] and then printed onto filter paper using a wax printer (Xerox ColorQube 8570). The printed devices were placed on a hot plate (123 °C) for 5 min, which caused the wax to permeate throughout the paper, forming the 3D—hydrophobic barriers to control liquid flow (Fig. 1(a)). Silver nitrate ($AgNO_3$) and magnesium chloride ($MgCl_2$) were pre-deposited into the hydrophilic region (white color) as electrolyte for each of the half-cells, as specified in Figure 1(a). Barium chromate ($BaCrO_4$), an oxidation agent of magnesium metal was also pre-deposited. The treated magnesium foil was used as the anode electrode, and the treated silver foil was used as the cathode electrode in the galvanic cell.

Electrodes were affixed using an adhesive tape to the bottom layer of filter paper before folding and attaching the filter paper layers to one another using glue applied to the wax surface (Figs. 1(a) and 1(b)). The assembled paper-based battery chip was pressed using a three pound block for half day (Fig 1(c)). The battery did not require a separately configured salt bridge because the half-cells in paper-based battery are connected as shown Figs. 1(a) and 1(b): the electrolytes were pre-deposited on hydrophilic zone (white color) of the paper layer, when dissolved in water, the soaked layers of filter paper yield a U-shaped salt bridge-like resistance. The battery's dimensions were 20.00 mm width × 20.00 mm length × 1.00 mm thickness and the total weight was 0.50 g (Fig. 1(c)).

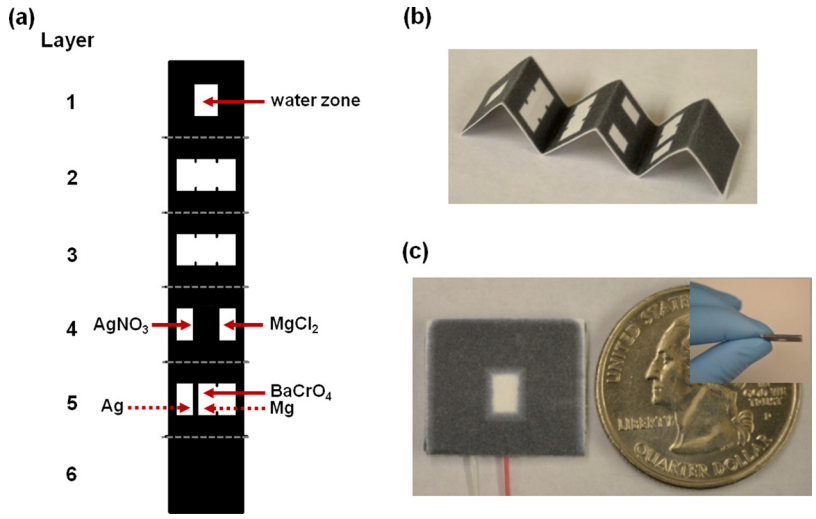

FIG. 1. Paper-based fluidic galvanic cell. (a) Schematic representation, (b) wax-printed Origami (paper folding) chip picture, and (c) top and side view of final assembled galvanic cell.

C. Galvanic cell performance

Performances of the paper-based fluidic galvanic cell was investigated using Gamry Potentiostat/ Galvanostat (Model: Reference 600, software: PWR 800), specifically the open circuit potential and discharge curves. All experiments were conducted in an aluminum Faraday cage. Discharge curves of paper-based fluidic galvanic cell were obtained using a constant load of current. The performances for red LED and UV-LED power output were also evaluated. The current and voltage were measured simultaneously using a Fluke digital multimeter.

D. Fluorescence assay

Fluorescence assays to detect ALPs were performed using a paper-based fluidic device consisting of a battery chip (with two galvanic cells with an in-serial connection), a UV-LED, and fluorescent assay components. A piece of transparent polyproplyene film covered the top of the UV-LED.

The phosphatase substrate fluoresces blue with a maximum excitation at 345 nm. Once the substrate's phosphate group is enzymatically removed via reaction with alkaline phosphatase, the resulting product is an intensely fluorescent green precipitate with a maximum emission at 530 nm.[24] Phosphatase substrate was diluted 20-fold in detection buffer. We loaded 160 μ distilled water to the inlet of the battery chip described above and then 8 μl of phosphatase substrate was added to the assay zone over 15 min. A picture (iPhone 4 S) of the assay zone was taken and analyzed using the Colour Detector Application (Nanospark version 1.5). Alkaline phosphatases (48 mU/ml) were then loaded onto the assay zone and another picture taken. A calibration curve was obtained using different alkaline phosphatase concentrations using a power supply to provide constant voltage; the voltage used (3.2 V (Fisher Scientific, U33020) was the same voltage obtained from a chip comprising two-galvanic cells in series in combination with the UV-LED and fluorescence assay region (see Figure 3(c)).

III. RESULTS AND DISCUSSION

Fig. 2 shows the performance results of a paper-based fluidic galvanic single cell. As shown in Fig. 2(a), the amount of the electrolytes were optimized to maximize the open circuit potential; the final optimized amount was 3.33 mg for $MgCl_2$ and 3.57 mg for $AgNO_3$ (dashed-line box in Fig. 2(a)).

As shown in Fig. 2(b), the open circuit potential of the single galvanic cell was maintained at 2.2 V for 1 h after loading 80 μl of distillated water. Fig. 2(c) shows a discharge curve with constant current density, 300 μA, for 1 h (Galvanostatic test). The potential immediately

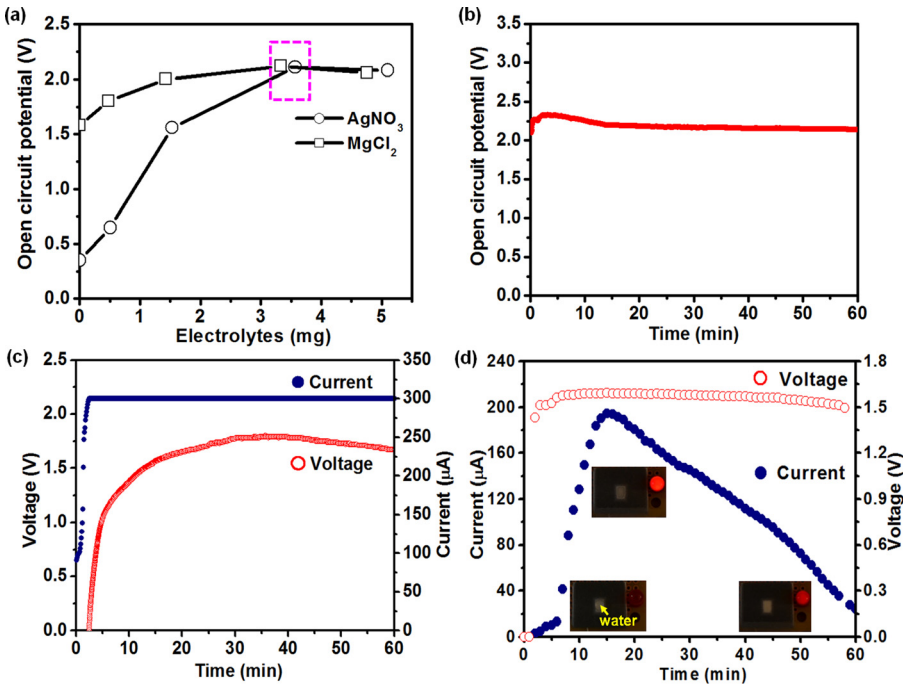

FIG. 2. Paper-based fluidic galvanic single cell. (a) Electrolytes effect between anode and cathode. (b) Open circuit potential of single galvanic cell, (c) discharge curve at constant current 300 μA, and (d) measuring the relative current and running voltage of light produced by the red LED in the single galvanic cell.

increased after 80 μl of distilled water was loaded to the inlet on the top of paper chip and the potential was maintained at 1.6 V for 1 h. Fig. 2(d) shows that red LED (which requires a minimum of 50 μA to light) was successfully lit even as the voltage decreased to 1.5 ± 0.1 V and was maintained for 1 h while the current slowly decreased. Another drop of water added at the end of the first hour led to a recovery of the current and red LED was on again (Fig. S3 in the supplementary material).[23] Even though we did not show the result, LED was on more than 5 h as long as water provided and until magnesium dissolve.

The electrochemical reaction for the water-operated paper microfluidic battery at the magnesium anode (oxidation) and silver cathode (reduction) are represented by Eqs. (1) and (2), respectively,[25–27]

$$\text{Anode} \qquad \mathrm{Mg} + 2\mathrm{e}^- \rightarrow \mathrm{Mg}^{2+}, \tag{1}$$

$$\text{Cathode} \qquad 2\mathrm{AgNO_3} + 2\mathrm{e}^- \rightarrow 2\mathrm{Ag} + 2\mathrm{NO_3^-}, \tag{2}$$

$$\text{Overall} \qquad \mathrm{Mg} + 2\mathrm{AgNO_3} \rightarrow \mathrm{Mg(NO_3)_2} + 2\mathrm{Ag}. \tag{3}$$

Because Mg is an active material, a side reaction between the Mg anode and the electrolyte in the drenched paper can occur according to the following equation:

$$\mathrm{Mg} + 2\mathrm{H_2O} \rightarrow \mathrm{Mg(OH)_2} + \mathrm{H_2}. \tag{4}$$

While this reaction may occur in theory, we did not observe hydrogen bubble evolution in the experimental set up, using a microCT to monitor the reaction (see supplementary material Fig. S4, video S1).[23]

Based on the standard reduction potential difference between magnesium, −2.37 V and silver, 0.08 V,[28] the theoretical potential of this paper-based galvanic cell is 3.17 V. Experimentally, the measured potential was 2.20 V. Without being bound by theory, it is possible that formation of magnesium hydroxide on the magnesium surface[29] and Ohmic polarization

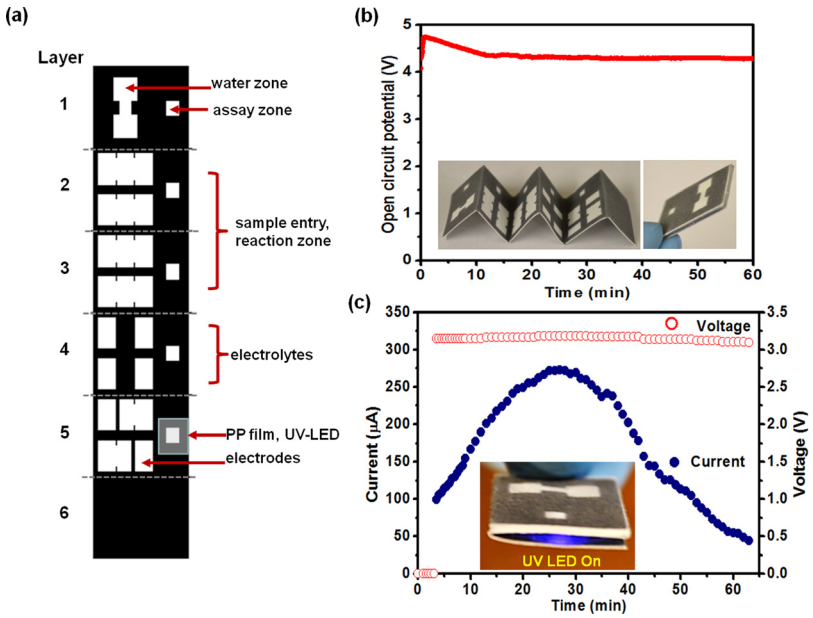

FIG. 3. Paper-based microfluidic device consisting of a battery chip (two galvanic cells in-serial connection, UV-LED, and fluorescent assay components): (a) Origami design for paper-based device, (b) graph of open circuit potential over the first hour, (c) graph of the power-output (current and voltage) from a two-series galvanic cell in serial connection with a load comprising a surface-mounted UV LED ($\lambda = 365$ nm).

based on solution resistance[30,31] are factors contributing to the decreased potential. The calculated power density of the single galvanic cell is 3.00 mW/cm^2 (Fig. 2(c)).

Figure 3 shows schematic design of a paper based microfluidic device consisting of a battery chip (two-galvanic cells in-serial connection) integrated with surface mounted UV-LED (see video S2)[23] and fluorescent assay components. The paper-based design consists of six layers; (1) inlet zone, (2) sample entry, (3) reaction zone, (4) pre-deposited electrolytes, (5) UV-LED/electrode integrated layer, and (6) bottom hydrophobic layer. The assembled paper-based microfluidic chip was 25.60 mm wide × 19.20 mm long × 2.20 mm thick (Fig. 3(b) inset). As shown in Fig. 3(b), the open circuit potential of the two-galvanic cell in serial connection initially increased and then stabilized at 4.30 V. Upon loading of 160 μl distilled water to the inlet (water zone) of the battery, emission from the surface-mounted UV-LED ($\lambda = 365$ nm) was observed; current and voltage were measured over time (Fig. 3(c)). The maximum current was 260 μA while the voltage remained essentially constant at 3.2 V (maximum power, 0.83 mW). Compared with the results from Thom *et al.*,[10] which need 24 cells to run a UV-LED, magnesium anode based paper microfluidic battery provided superior performance.

TABLE I. Comparison of paper-based microfluidic battery reported in literature.

Anode	Cathode	Open circuit potential (V)	Max. current (power out, μA)	Life time (min)	Literature
Mg	Ag	2.2 (1-cell) 4.2 (2-cells)	260 (UV-LED, 2-cells)	~60	This article
Al	Ag	1.3 (1-cell) 5.0 (24-cells)	300[a] (UV-LED, 24-cells)	~60	Ref. 10
Al	Cu	0.82 (1-cell) 5.0 (8-cells)	500 (Regular LED, 8-cells)	~65	Ref. 32

[a]Estimated from supplementary material of Ref. 10.

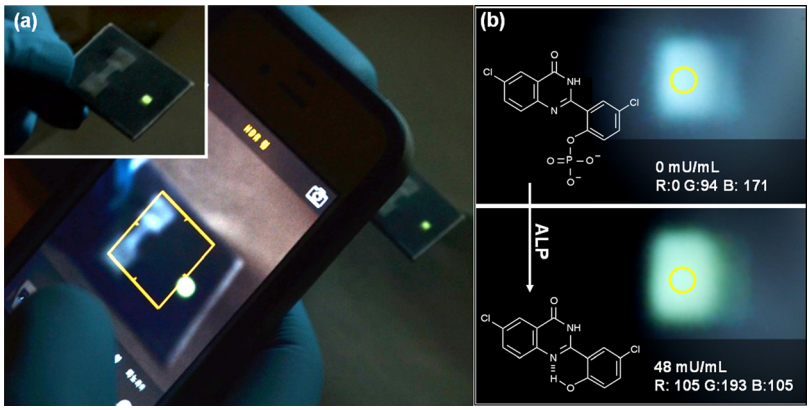

FIG. 4. A fluorescent assay-based alkaline phosphatase detection using a paper-based microfluidic device; (a) iPhone 4S photograph of fluorescent assay-based alkaline phosphatase detection, (b) colorimetric analysis of the photograph of the fluorescence from alkaline phosphatase detection (photographs show blue color before adding alkaline phosphatase (top picture) and green color after adding alkaline phosphatase (bottom picture)).

Table I shows the comparison of paper-based microfluidic battery reported in literatures. Paper-based battery based on Mg anode provides higher power density (3.0 mW/cm^2), enough to run bioanalytical devices.

Figure 4 demonstrates the proof-of- concept that a paper-based microfluidic device can be used to monitor a fluorescent assay. A battery comprising two-galvanic cells connected in-serial was able to operate a UV-LED ($\lambda = 365$ nm) to detect alkaline phosphatase based on a color evaluation using an iPhone 4S (Fig. 4(a)). Fig. 4(b), (top and bottom photographs) shows a change from a weak blue color at 0 mU/ml enzyme concentration to green color at 48 mU/ml enzyme concentration. The green color intensity was measured using Colour Detector (Nanospark version 1.5) an iPhone application.

Figure 5 shows a calibration curve of alkaline phosphatase concentration versus the intensity of green light from the LED, as evaluated by Colour Detector. The results show a typical calibration curve, which (1) starts 85 color intensity at 0 mU/ml, (2) be gradually increased and then (3) is slowly saturated. Dynamic range as well as detection limits of this device can be improved by (1) increasing of the UV-LED light intensity by increasing power such as four cells, (2) controlling sample volume at assay zone, (3) using better color detection software.

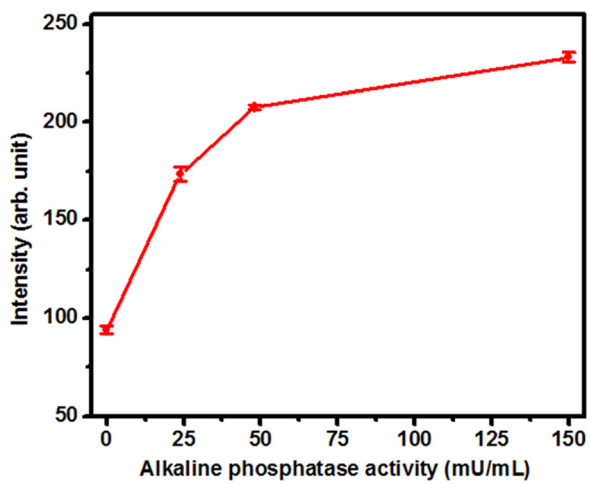

FIG. 5. Calibration curve of alkaline phosphatase concentration versus green intensity measured by iPhone application.

IV. CONCLUSION

We have developed paper-based microfluidic battery using Mg anode that has a high power density. This disposable battery was shown the possibility for point of care devices interfaced smart phone App. This has a number of key advantages: (1) easy high power generation, (2) extremely low production costs, (3) high-throughput fabrication, (4) easy to dispose, (5) fast/self high-surface-to-volume ratio, and (6) self powering bio/chemical reaction/detection regardless of heavy and expensive extra facilities. Therefore, this high powered paper based galvanic cell is suitable for disposable devices such as portable diagnostics, bio/chemical sensor, and emergency power patch. It will be useful to have an electrochemical biosensor as a point-of-care device that can be developed several biomarkers at a relatively low cost.

ACKNOWLEDGMENTS

This research was partially supported by NSF Engineering Research Center for Revolutionizing Metallic Biomaterials (ERC-RMB) at North Carolina A&T State University. The authors also give special thanks to Dr. Laura Collins, Dr. Boyce Collins, and Dr. Peter Seoane for reading the manuscript, imaging with CT, and overall guidance.

[1]R. H. Müller and D. L. Clegg, Anal. Chem. **21**, 1123 (1949).
[2]X. Li, D. R. Ballerini, and W. Shen, Biomicrofluidics **6**, 011301 (2012).
[3]B. Chumo, M. Muluneh, and D. Issadore, Biomicrofluidics **7**, 064109 (2013).
[4]I. N. Katis, J. A. Holloway, J. Madsen, S. N. Faust, S. D. Garbis, P. J. S. Smith, D. Voegeli, D. L. Bader, R. W. Eason, and C. L. Sones, Biomicrofluidics **8**, 036502 (2014).
[5]S. Wang, L. Ge, Y. Zhang, X. Song, N. Li, S. Ge, and J. Yu, Lab Chip **12**, 4489 (2012).
[6]H. Noh and S. T. Phillips, Anal. Chem. **82**, 8071 (2010).
[7]H. Liu and R. M. Crooks, J. Am. Chem. Soc. **133**, 17564 (2011).
[8]A. C. Siegel, S. T. Phillips, M. D. Dickey, N. Lu, Z. Suo, and G. M. Whitesides, Adv. Funct. Mater. **20**, 28 (2010).
[9]Q. Cheng, Z. Song, T. Ma, B. B. Smith, R. Tang, H. Yu, H. Jiang, and C. K. Chan, Nano Lett. **13**, 4969 (2013).
[10]N. K. Thom, K. Yeung, M. B. Pillion, and S. T. Phillips, Lab Chip **12**, 1768 (2012).
[11]J. P. Esquivel, F. J. Del Campo, J. L. Gómez de la Fuente, S. Rojas, and N. Sabaté, Energy Environ. Sci. **7**, 1744 (2014).
[12]P. Yager, T. Edwards, E. Fu, K. Helton, K. Nelson, M. R. Tam, and B. H. Weigl, Nature **442**, 412 (2006).
[13]J. O. Besenhard and M. Winter, ChemPhysChem **3**, 155 (2002).
[14]R. Udhayan, N. Muniyandi, and P. B. Mathur, Br. Corros. J. **27**, 68 (1992).
[15]D. Aurbach, Z. Lu, A. Schechter, Y. Gofer, H. Gizbar, R. Turgeman, Y. Cohen, M. Moshkovich, and E. Levi, Nature **407**, 724 (2000).
[16]H. S. Kim, T. S. Arthur, G. D. Allred, J. Zajicek, J. G. Newman, A. E. Rodnyansky, A. G. Oliver, W. C. Boggess, and J. Muldoon, Nat. Commun. **2**, 427 (2011).
[17]B. Peng, J. Liang, Z. Tao, and J. Chen, J. Mater. Chem. **19**, 2877 (2009).
[18]Y. Nuli, Z. P. Guo, H. K. Liu, and J. Yang, Electrochem. Commun. **9**, 1913 (2007).
[19]W. Y. Li, C. S. Li, C. Y. Zhou, H. Ma, and J. Chen, Angew. Chem., Int. Ed. **45**, 6009 (2006).
[20]J. L. Robinson, "Magnesium cells," in *The Primary Battery*, edited by N. C. Cahoon and G. W. Heise (Wiley-Interscience, New York, 1976), Vol. 2, Chap. 2.
[21]M. J. Favus, *Primer on the Metabolic Bone Diseases and Disorders of Mineral Metabolism* (American Society for Bone and Mineral Research, Washington, DC, USA, 2006), p. 129.
[22]R. B. McComb, G. N. Bowers, and S. Posen, *Alkaline Phosphatase* (Plenum Press, New York, USA, 1979).
[23]See supplementary at http://dx.doi.org/10.1063/1.4894784 for a detailed description of Fig. S1, Fig. S4, video S1, and video S2.
[24]http://www.lifetechnologies.com/us/en/home/life-science/cell-analysis/labeling-chemistry/fluorescence-spectraviewer.html#product=E6601, (2014): This website can provide an excitation/emission wavelength of ELF97 fluorophore used in the fluorescence assay of this article.
[25]S. Firas, K. B. Lee, and L. Lin, Sens. Actuators, A **111**, 79 (2004).
[26]*Handbook of Batteries*, 2nd ed., edited by D. Linden (McGraw-Hill, New York, 1995).
[27]R. F. Koontz and R. D. Lucero, in *Handbook of Batteries* (McGraw-Hill, 2002), Chap. 17.
[28]Standard electrode potential, see http://en.wikipedia.org/wiki/Standard_electrode_potential_(data_page).
[29]Y. Yun, Z. Dong, N. Lee, Y. Liu, D. Xue, X. Guo, J. Kuhlmann, A. Doepke, H. B. Halsall, W. Heineman, S. Sundaramurthy, M. J. Schulz, Z. Yin, V. Shanov, D. Hurd, P. Nagy, W. Li, and C. Fox, Mater. Today **12**, 22 (2009).
[30]J. M. Sherfey and A. Brenner, J. Electrochem. Soc. **105**, 665 (1958).
[31]R. P. Ramasamy, C. Feger, T. Strange, and B. N. Popov, J. Appl. Electrochem. **36**, 487 (2006).
[32]S.-S. Chen, C.-W. Hu, I.-F. Yu, Y.-C. Liao, and J.-T. Yang, Lab Chip **14**, 2124 (2014).